Single-Phase Bidirectional Three-Level T-Type Inverter

Min-Kwon Yang and Woo-Young Choi
Division of Electronic Engineering
Chonbuk National University
Jeonju, South Korea
Email: wychoi@jbnu.ac.kr

***Abstract*—This paper proposes a single-phase bidirectional three-level T-type inverter. The proposed inverter has a T-type switching leg and a half-bridge switching leg. The T-type switching leg operates at high switching frequency with sinusoidal pulse width modulation. The half-bridge switching leg operates at the grid frequency according to the voltage polarity of the grid. Due to the three-level switching operation of the proposed inverter, it provides the advantages of low voltage stress, reduced switching loss, and low harmonic components for the single-phase gird-tied applications. The proposed inverter is introduced by describing its circuit configuration, switching technique, operation modes, and control scheme. A 1.0 kW prototype has been designed and experimentally tested to verify the performance of the proposed inverter.**

I. INTRODUCTION

Grid-tied energy storage systems require a high performance bidirectional inverter to transfer the electrical power between the grid and the energy storage devices [1]. The bidirectional inverter controls the bidirectional power flow and improves the power quality of the system [2]. To design the bidirectional inverter, the inverter performances should be considered for higher power efficiency and higher power density.

Up to now, various single-phase transformerless inverters have been suggested [3]-[5]. Popular ones are H5, HERIC, and parallel buck inverters. By clamping the common-mode voltage as constant [3], H5 inverter and HERIC inverter have minimized the ground leakage current. By clamping the parasitic capacitor voltage as constant [4], the parallel buck inverters have been adopted for the grid-tied transformerless inverters. However, all they use a two-level power switching circuit where all power switches should withstand the full dc-link voltage when they are turned off [5]. When the inverter operates under a hard switching condition, switching losses become larger as the switching frequency and the rated power level are increased. In order to reduce switch voltage stresses, the half-bridge-based three-level inverters have been studied [6]. Although the switch voltage stresses can be reduced by half, they require doubling the dc-link voltage, compared to the full-bridge inverter. For example, a dc-link voltage of 700 V is required for 220 V_{rms} single-phase products.

To solve the above-mentioned drawbacks, this paper suggests a single-phase bidirectional inverter using the T-type switching circuit. Fig. 1 shows the circuit diagram of the proposed inverter. The proposed inverter has a T-type switching leg and a half-bridge switching leg. The T-type switching leg operates at high switching frequency with sinusoidal pulse width modulation. The half-bridge switching leg operates at the grid frequency according to the voltage polarity of the grid. Due to the three-level switching operation of the proposed inverter, it provides the advantages of low voltage stress, reduced switching loss, and low harmonic components for the single-phase gird-tied applications. The proposed inverter is introduced by describing its circuit configuration, switching technique, operation modes, and control scheme. A 1.0 kW prototype has been designed and experimentally tested to verify the performance of the proposed inverter.

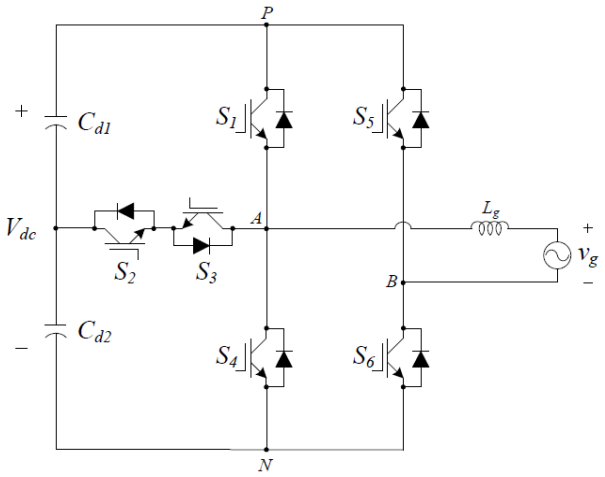

Fig. 1. Circuit diagram of the proposed inverter.

II. PROPOSED INVERTER

A. Switching States

Fig. 1 shows the circuit diagram of the proposed inverter. It has two dc-link capacitors (C_{d1}, C_{d2}), six power switches (S_1 ~ S_6), and a filter inductor (L_g). S_1 ~ S_4 operate with a high-frequency switching period. A sinusoidal pulse-width modulation is applied to S_1 ~ S_4 according to the switching

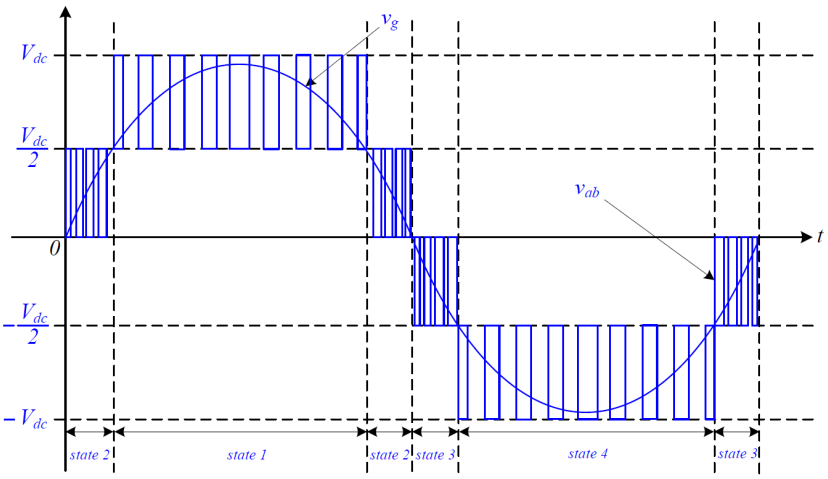

Fig. 2. Waveform diagrams for v_{AB} and v_g according to the switching states.

states. S_1 (S_2) and S_3 (S_4) operate complementarily each other, respectively. S_5 and S_6 operate as a line-frequency switching period. It is assumed that $V_{d1} = V_{d2}$ and $V_{dc} = V_{d1} + V_{d2}$. v_g is the grid voltage as $v_g = V_g \sin wt$ where V_g and w are the peak value and the angular frequency of v_g, respectively.

The proposed inverter has two operation modes: rectifier mode and inverter mode. When it operates in the rectifier mode, it transfers the electrical power from v_g to V_{dc}. When it operates in the inverter mode, it transfers the electrical power from V_{dc} to v_g. Because both operation modes can be similarly explained, the circuit operation for the inverter mode is only described for one switching period T_s. The proposed inverter has six switching states which results in five voltage levels (V_{dc}, $V_{dc}/2$, 0, $-V_{dc}/2$, $-V_{dc}$) for v_{AB}. Then, the switching states can be determined by the five voltage levels because v_g can be divided into four sections as state 1 ($V_{dc}/2 < v_g < V_{dc}$), state 2 ($0 < v_g < V_{dc}/2$), state 3 ($-V_{dc}/2 < v_g < 0$), and state 4 ($-V_{dc} < v_g < -V_{dc}/2$). Fig. 2 shows the waveform diagrams for v_{AB} and v_g according to the switching states. When v_g is positive, S_6 is turned on and S_5 is turned off. When v_g is negative, S_5 is turned on and S_6 is turned off. Because S_1 (S_2) and S_3 (S_4) operate complementarily each other, respectively, two duty cycles are needed to control the proposed inverter. D_{S1_SS} is the steady-state duty cycle of S_1. D_{S2_SS} is the steady-state duty cycle of S_2.

B. Inverter Operations

In switching state 1, S_1 and S_3 operate with a high-frequency. S_2 is turned on and S_4 is turned off. When S_1 is turned on, i_{Lf1} flows through S_1 and S_2. It results in a negative voltage $v_g - V_{dc}$ across L_{f1} and L_{f2}. When S_1 is turned off, i_{Lf1} flows through S_3. It results in a positive voltage $v_g - V_{dc}/2$ across L_{f1} and L_{f2}. By applying the volt-second balance rule to L_{f1} and L_{f2} for T_s, the steady-state duty cycle D_{S1_SS} of S_1 can be obtained as

$$(v_g - V_{dc})D_{S1\_SS} + (v_g - \frac{V_{dc}}{2})(1 - D_{S1\_SS}) = 0 . \quad (1)$$

By rearranging (1),

$$D_{S1\_SS} = \frac{2v_g}{V_{dc}} - 1, \qquad \text{for switching state 1} \quad (2)$$

On the other hand, the steady-state duty cycle D_{S2_SS} of S_2 can be represented as

$$D_{S2\_SS} = 1, \qquad \text{for switching state 1} \quad (3)$$

For the rest of the switching states, the volt-second balance rule can be applied to L_{f1} and L_{f2} for T_s, which results in the following steady-state duty cycles as

$$D_{S1\_SS} = 0, \; D_{S2\_SS} = \frac{2v_g}{V_{dc}}, \text{ for switching state 2} \quad (4)$$

$$D_{S1\_SS} = \frac{2v_g}{V_{dc}} + 1, \; D_{S2\_SS} = 1, \text{ for switching state 3} \quad (5)$$

$$D_{S1\_SS} = 0, \; D_{S2\_SS} = \frac{2v_g}{V_{dc}} + 2, \text{ for switching state 4} \quad (6)$$

C. Control Schemes

For the grid-tied bidirectional operation of the proposed inverter, the grid current i_g should be controlled instantaneously. For each switching state, a transient duty cycle should be added to the steady-state duty cycle. In case of the switching state 1, the average voltage equation for L_g during T_s can be represented as

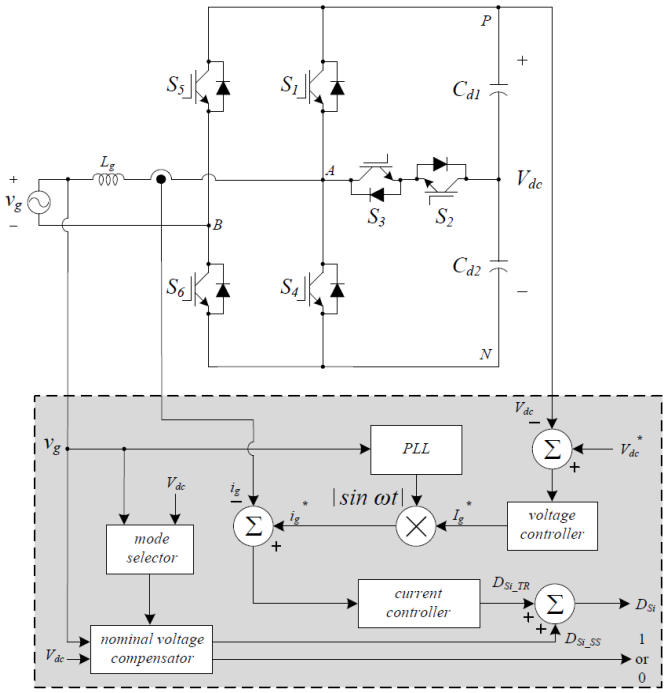

Fig. 3. Control diagram of the proposed inverter.

$$(v_g - V_{dc})D_{S1} + (v_g - \frac{V_{dc}}{2})(1 - D_{S1}) = L_g \frac{\Delta i_g}{T_s} \quad (7)$$

where D_{S1} is the final duty cycle of S_1. Δi_g is the variation of the grid current i_g. By rearranging (7),

$$D_{S1} = D_{S1\_SS} + D_{S1\_TR} = (\frac{2v_g}{V_{dc}} - 1) - \frac{2L_g \Delta i_g}{V_{dc} T_s}, \quad \text{for switching state 1} \quad (8)$$

where D_{S1_TR} is the transient duty cycle of S_1 as

$$D_{S1\_TR} = -\frac{2L_g \Delta i_g}{V_{dc} T_s}, \quad \text{for switching state 1} \quad (9)$$

D_{S1_SS} provides a fast tracking of the fundamental component of the grid current i_g. D_{S1_TR} makes the grid current track the grid current reference i_g^*. For the rest of the switching states, the transient duty cycle can be derived for each switch. Fig. 3 shows the control diagram of the proposed inverter. The proposed inverter performs the bidirectional power control between v_g and V_{dc}. As V_{dc} varies when a power difference occurs, V_{dc} can be regulated by controlling the transferred power reflected by i_g. A PI controller regulates V_{dc}, which generates the grid current reference i_g^*. By changing the sign of i_g^*, the proposed inverter controls the bidirectional power flow between v_g and V_{dc}.

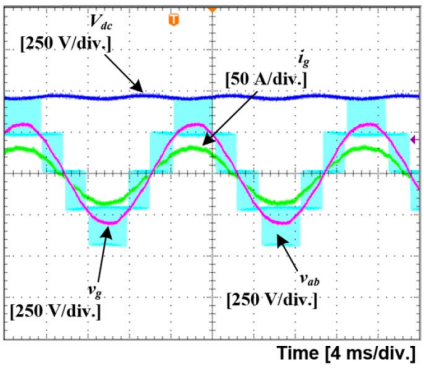

Fig. 4. Experiment results for the rectifier mode

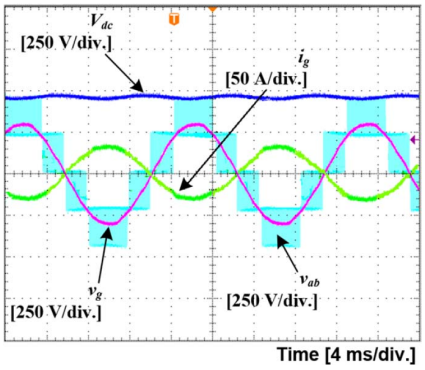

Fig. 5. Experiment results for the inverter mode.

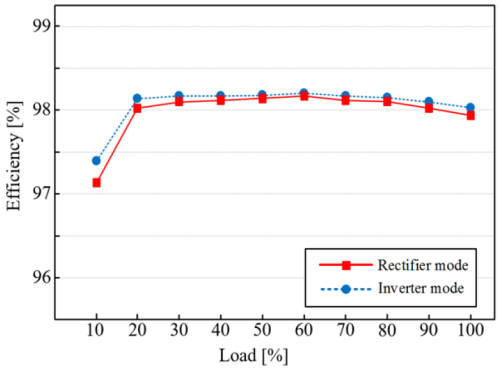

Fig. 6. Measured power efficiency curves.

III. Experimental Results

A 1.0 kW prototype has been designed and experimentally tested to verify the performance of the proposed inverter. v_g is 60 Hz/220 V_{rms}. V_{dc} is 380 V. T_s is 50 µsec. The passive circuit components are selected as L_g = 2.0 mH and C_{d1} = C_{d2} = 440 µF. Fig. 4 shows the experiment results when the proposed inverter operates for the rectifier mode. Fig. 5 shows the experiment results when the proposed inverter operates for the inverter mode. Fig. 6 shows the measured power efficiency curves for different output load conditions. The proposed inverter achieves the efficiencies of 98.1 % and 97.7 % for the

inverter and rectifier modes, respectively at the rated load condition.

IV. Concluding Remarks

In this paper, a single-phase three-level T-type bidirectional inverter has been suggested. The proposed inverter has a T-type switching leg and a half-bridge switching leg. The T-type switching leg operates at high switching frequency with sinusoidal pulse width modulation. The half-bridge switching leg operates at the grid frequency according to the voltage polarity of the grid. Due to the three-level switching operation of the proposed inverter, it provides the advantages of low voltage stress, reduced switching loss, and low harmonic components for the single-phase gird-tied applications. The proposed inverter has been introduced by describing its circuit configuration, switching technique, operation modes, and control scheme. Experimental results based on a 1.0 kW prototype system have been discussed to verify the performance of the proposed inverter.

Acknowledgment

This study has been supported by the grants of National Research Foundation of Korea (NRF-6R1D1A3B03932350) and Small and Medium Business Administration of Korea (C0445037).

References

[1] T.F. Wu, C. H. Chang, L. C. Lin, Y. C. Chang, and Y. R. Chang, "Two-phase modulated digital control for three-phase bidirectional inverter with wide inductance variation," *IEEE Trans. Power Electron*., vol. 28, no. 4, pp. 1598-1607, Apr. 2013.

[2] M. P. Akter, S. Mekhilef, N. M. L. Tan, and H. Akagi, "Modified model predictive control of a bidirectional AC-DC converter based on lyapunov function for energy storage systems," *IEEE Trans. Ind. Electron*., vol. 63, no. 2, pp. 704-715, Feb. 2016.

[3] W. Li, Y. Gu, H. Luo, W. Cui, X. He, and C. Xia, "Topology review and derivation methodology of single-phase transformerless photovoltaic inverters for leakage current suppression," *IEEE Trans. Power Electron*., vol. 62, no. 7, pp. 4537-4551, Jul. 2015.

[4] T. K. S. Freddy, N. A. Rahim, W. P. Hew, and H. S. Che, "Comparison and analysis of single-phase transformerless grid-connected PV inverters," *IEEE Trans. Power Electron*., vol. 29, no. 10, pp. 5358-5369, Oct. 2014.

[5] S. V. Araujo, P. Zacharias, and R. Mallwitz, "Highly efficient single-phase transformerless inverters for grid-connected photovoltaic systems," *IEEE Trans. Ind. Electron*., vol. 57, no. 9, pp. 3118-3128, Sep. 2010.

[6] R. Gonzalez, E. Gubia, J. Lopez, and L. Marroyo, "Transformerless single-phase multilevel-based photovoltaic inverter," *IEEE Trans. Ind. Electron*., vol. 55, no. 7, pp. 2694-2702, Jul. 2008.